Industrial Crops & Products 132 (2019) 292–300

Contents lists available at ScienceDirect

Industrial Crops & Products

journal homepage: www.elsevier.com/locate/indcrop

Lab-scale structural insulated panels with lignin-incorporated rigid polyurethane foams as core

Xuefeng Zhang[a,*], Yunsang Kim[a], Thomas L. Eberhardt[b], Rubin Shmulsky[a,*]

[a] Department of Sustainable Bioproducts, Mississippi State University, Starkville, MS, 39762, USA
[b] USDA Forest Service, Forest Products Laboratory, Madison, WI 53726, USA

ARTICLE INFO

Keywords:
Lignin
Structural insulated panel
Compressive strength and modulus
Bonding strength
Shear strength
Flexural strength

ABSTRACT

Lab-scale structural insulated panels (SIPs), using lignin-incorporated rigid polyurethane (RPU) foams as the thermal insulation core, were fabricated and characterized. The RPU foams incorporating surface-modified lignin were sandwiched between two oriented strand board (OSB) sheets to produce lignin-incorporated SIPs with nominal dimensions of 350 × 350 × 46 mm^3. In comparison to the reference RPU foam without lignin, the lignin-incorporated RPU foams exhibited progressively higher thermal stabilities coinciding with lignin amount, but similar thermal conductivity (~24.5 $mW{\cdot}m^{-1}K^{-1}$) and water absorption (~0.018 g/cm^3). The bonding, shear, and flexural strength of lignin-incorporated SIPs were 150–210 kPa, 110–150 kPa, and 3–4 MPa, respectively, which were similar to that of reference (no lignin control) SIP. Lignin-incorporated RPU foams and SIPs with 5%–15% lignin addition amount exhibit better performance than the reference RPU foam and SIP. We attribute overall enhancements in thermal and mechanical properties of the lignin-incorporated RPU foams, and the corresponding SIPs, to the surface-modified lignin, serving as a reactive crosslinker with ample chemical interaction to polyisocyanates during the formation of RPU foams.

1. Introduction

Structural insulated panels (SIPs), made by sandwiching a thick insulating layer between two structural face layers, are used worldwide as an energy conservation composite for residential and commercial buildings (Jing and Raongjant, 2013). The competitiveness of SIPs in the multistory wooden structures industry is made possible by the prefabrication of SIPs in a factory to required specifications; this results in less construction waste and significant time-savings through the installation of whole wall systems during onsite structure assembly. SIPs are also lightweight and their energy efficiency results in energy savings of 50–60% (Bartel, 2018). The annual market for SIPs in the US was estimated to be $350-525 million in 2007 with a 4–12% annual growth rate (FAS, 2010). For residential buildings, the most commonly used face layer in SIPs is oriented strand board (OSB) and materials used for the core are rigid polystyrene (RPS) or rigid polyurethane (RPU) foams. RPU foams are highly cross-linked and closed-cell thermoset polymers which are usually synthesized through a polyaddition reaction between –NCO rich polyisocyanates and −OH rich polyols. Generally, RPU foams have the advantages of high thermal insulating capability and high durability over RPS foams (Choi et al., 2018). Besides, unlike RPS foams, the forming of RPU foams can be carried out directly between two OSB panels to produce SIPs without the use of adhesives to bond the insulating-foam and face-OSB layers. Despite their outstanding properties, the use of petroleum-based polyols and polyisocyanates for the production of RPU foams can be a concern due to the depletion of fossil fuel resources and possible environmental issues arising from low biodegradability and compostability of petroleum-based materials (Amaral et al., 2012). Therefore, applying bio-based materials for the production of RPU foams as well as SIPs would lead to a reduction of the environmental footprint of petroleum-based materials and resources (Kirpluks et al., 2018; Li et al., 2017; Septevani et al., 2017).

Lignin is one of the three major components of lignocellulosic biomass, which accounts for approximately 10–35 wt% of the 200 billion tons of total global biomass produced annually (Zhang et al., 2017). Although a large amount of (70 million tons/year) lignin is available from pulping industries as a byproduct, the large scale application of lignin is still limited (Zhang et al., 2018a 2018b). As a renewable and biodegradable biopolymer, lignin has attracted global interest in the polymer industry for both economic and environmental reasons. Many attempts have been made to utilize lignin as renewable polyol feedstock to produce RPU foams in order to supersede the use of petroleum-based polyols (Bernardini et al., 2015; Carriço et al., 2016; Cateto et al., 2008, 2014; Li and Ragauskas, 2012; Luo et al., 2013; Nadji et al., 2005). In

* Corresponding author.
E-mail addresses: njfuxf@gmail.com (X. Zhang), rs26@msstate.edu (R. Shmulsky).

https://doi.org/10.1016/j.indcrop.2019.02.035
Received 8 October 2018; Received in revised form 10 February 2019; Accepted 16 February 2019
Available online 22 February 2019

these attempts, lignin was used either directly (without modification) or after a chemical modification (*i.e.*, liquefaction or oxypropylation). The former method is simple but usually weakens the mechanical strength of RPU foams (Pan and Saddler, 2013; Xue et al., 2014; Gómez-Fernández et al., 2017), while the latter method could maintain the good mechanical strength of RPU foams but increases the production cost (Hayati et al., 2018; Zhang et al., 2018c). Applying unmodified lignin for RPU foam production could be attractive for industries due to its potential economic benefit.

Two obstacles associated with direct incorporation of unmodified lignin for RPU foam production are: 1) limited miscibility of lignin with polyols due to their difference in polarity and 2) low reactivity of lignin to isocyanates due to the high phenolic OH content and the limited accessibility of the phenolic OH groups from steric hindrance. The first obstacle is believed to cause the aggregation of lignin particles in the cellular structure of RPU foam and diminish its mechanical strength. To overcome this issue, Hayati et al. (2018) have applied a high-temperature dispersion method to solubilize industrial lignin (up to 10%) in a polyether polyol mixture and have used lignin/polyol dispersion to produce RPU foams. In comparison to the conventional room-temperature dispersion, high-temperature (120 °C) was found to be effective in the dissolution and disaggregation of lignin in the polyether polyol, thereby improving the thermal insulation property (up to 5%) and compressive strength (up to 4%) of RPU foams. Although the improvement in RPU foams' properties is marginal, the high-temperature dispersion method can be a simple and effective strategy for the production of lignin-incorporated RPU foam. On the other hand, the second obstacle caused the low crosslink density of lignin-incorporated RPU foams because lignin mainly served as a filler other than a reactive polyol. This is because the foaming reaction is a rapid process that usually completed in a few tens of seconds. Even if the foam is cured after the completed reaction between polyols and isocyanates, lignin particles will likely be trapped in the cellular wall and remain unreacted.

The direct incorporation of lignin for RPU foam production with maintaining a reasonable crosslink density remains challenging. Therefore, this study investigates an alternative strategy for increasing the crosslink density of lignin-incorporated RPU foams. We have reported a simple surface functionalization process to utilize lignin as a petrochemical polyol substitute for the preparation of RPU foams (Zhang et al., 2018c). Our approach was to modify the surface of lignin with polyisocyanates at a moderate temperature in order to increase the interaction between lignin and polyisocyanates as well to enhance the dispersion and disaggregation of lignin. On the other hand, despite lignin-incorporated RPU foams with different densities and mechanical properties were prepared by many studies, there are no reports for lignin-incorporated RPU foams used in practical applications such as the fabrication of SIPs. The mechanical properties of SIPs are not only affected by the individual mechanical properties of the components (core foam, OSB), but also by the interfaces between core foam and each of the two OSB layers. Therefore, it is necessary to fabricate lignin-incorporated SIPs and test their mechanical properties because the addition of lignin may affect the core foam and OSB interface, and thus affect the mechanical properties of a SIP.

In this study, the effects of lignin addition on the microstructure, thermal conductivity, and thermal stability of RPU foams were examined. The mechanical performance of SIPs containing lignin-incorporated RPU foams as the thermal insulation core, such as compressive, bonding, shear, and flexural properties, were also investigated. To the best of our knowledge, this is the first study applying lignin-incorporated RPU foams in the fabrication of SIPs.

2. Experimental

2.1. Materials

Kraft lignin (Indulin AT) supplied from Ingevity (North Charleston, SC, USA), and the lignin powder was milled in a coffee burr mill to pass through a 90 μm sieve and oven dried (103 °C for 24 h) prior to use. Lignin was also further characterized for its ash content, hydroxyl content, and molecular weight (Fig. S1 in Supplementary information: SI). Lignin ash content was measured to be 3.62 wt% following ASTM D1102. Lignin total hydroxyl content was 5.33 mmol/g (hydroxyl value: 299 mg KOH/g), in which aliphatic hydroxyl, phenolic hydroxyl, and carboxylic-related hydroxyl contents were 2.21, 2.89, and 0.22 mmol/g, respectively (Fig. S2). Lignin molecular weight (Mw) and polydispersity index (Mw/Mn: PDI) were found to be 4825 g/mol and 5.77, respectively. From this data, the average functionality was calculated to be 4.45. Commercial 23-015 low-density rigid pour system was purchased from NCFI Polyurethanes (Mount Airy, NC, USA). The 23-015 consists of two parts. Part A is polyisocyanates mixture (pMDI, NCO content 7.61 mmol/g, viscosity 200 mPa·s), containing 46% diphenylmethane diisocyanate isomers and 54% polymeric diphenylmethane diisocyanate. Part B is a petroleum-based polyester polyol mixture (hydroxyl value 272 mg KOH/g, viscosity 1030 mPa·s), which contains 1% tertiary amine catalyst and 9% hydrofluorocarbon (HFC) blowing agent (a proprietary blend of HFC-245fa and HFC-365mfc). OSB (7/16 CAT PS2-10, 11 mm in thickness) was manufactured by Georgia-Pacific Corporation and purchased from a local retailer. Epoxy resin (635 Thin Epoxy System, epoxy and hardener volume ratio of 3:1) was purchased from US composites Inc. Other chemicals were purchased from Sigma-Aldrich as analytical grade and used as received.

2.2. Preparation of lignin-incorporated RPU foams and SIPs

Prior to the preparation of lignin-incorporated RPU foams and SIPs, the lignin was surface functionalized using pMDI *via* a prepolymerization treatment according to our established procedures (Zhang et al., 2018c). Briefly, the prepolymerization treatment was initiated by heating a mixture of lignin, pMDI, and silicone oil at 80 °C for 1 h under the N_2 atmosphere with stirring (see Scheme 1 for details). The temperature we used was 80 °C which was close to lignin's soft point but not high enough to cause the homopolymerization of pMDI. Lignin concentration in the mixture was up to 30%, which was respective to the mass of pMDI (as shown in Table 1). After the prepolymerization, the resultant mixture, which is termed as lignin-pMDI prepolymer, was cooled down to room temperature and used immediately for the preparation of RPU foams and SIPs. For the convenience of description, unless stated, the "lignin amount (%)" and "lignin content (%)" in this article refer to the weight fraction of lignin in relative to pMDI in the prepolymer.

The optimized mixture ratio of 1:1 (part A to part B in weight) was suggested from NCFI Polyurethanes, which was used for the preparation of reference RPU foam and SIP. For lignin-incorporated RPU foams and SIPs, the amount of foaming chemicals (part A and part B) kept to be the same and a predefined amount of lignin was added to it (Table 1). The NCO index of RPU foams (Table 1) was calculated from the following equation:

$$\text{NCO index} = [W_{pMDI} \times NCO_{pMDI} / (W_P \times OH_P + W_{Lig} \times OH_{Lig})] \times 100 \quad (1)$$

where W_{pMDI}, W_P, and W_{Lig} are the weight (g) of pMDI, polyol, and lignin, respectively; NCO_{pMDI} is NCO content of pMDI (7.61 mmol/g); OH_P and OH_{Lig} are the OH content of polyol (4.85 mmol/g) and lignin (5.33 mmol/g), respectively. The actual lignin content (ALC, %), which represents the weight fraction of lignin in RPU foams, was calculated using the following formula:

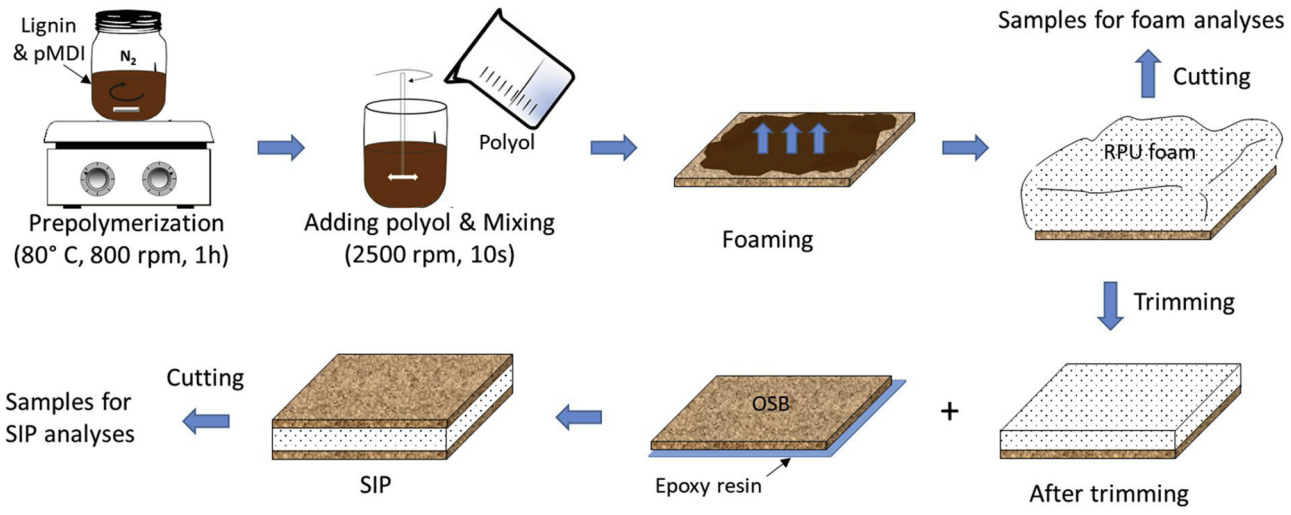

Scheme 1. The preparation of lignin-based RPU foams and SIPs.

$$ALC, \% = W_{Lig} / (W_P + W_{Lig} + W_{pMDI} + W_{Si\text{-}oil}) \quad (2)$$

where $W_{Si\text{-}oil}$ is the weight of silicone oil.

Our preliminary experiments found that direct pouring of the premixed RPU foam components (shown in Table 1) into the OSB mold (consisting of two OSB panels as faces on edge) resulted in non-uniform RPU foams, which produced SIPs with uneven core foam densities. To ensure the uniform core foam density of the as-prepared SIPs, a three-step fabrication process was employed: 1) formation of a free-rising RPU foam, 2) trimming of the RPU foam, and 3) gluing top-face OSB panel on top of the RPU foam, as shown in Scheme 1. Specifically, a predetermined amount of part B polyol (Table 1) was added into lignin-pMDI prepolymer and the mixture was stirred at 2500 rpm for 10 s. The resultant mixture was then immediately transferred onto an OSB (35×35 cm^2) panel and allowed to freely expand at room temperature to obtain an RPU foam that adhered to the OSB panel. The RPU foam was then cut into samples with various sizes for the analyses of cell structure, density, thermal conductivity, and water absorption. For the preparation of SIPs, the as-synthesized RPU foam from the previous step was trimmed to the size of OSB (35×35 cm^2) with a thickness of 26 mm. By gluing a top OSB layer on the surface of the trimmed RPU with epoxy resin, the lignin-incorporated SIP was obtained. The SIP was cut into samples with various sizes depending on the mechanical property being determined.

2.3. Characterization

2.3.1. Characterization of lignin-pMDI prepolymers

The viscosity of lignin-pMDI prepolymer was determined at 25 °C at a shear rate of 10 s^{-1} using an AR 1500EX (TA Instruments) rheometer, which is equipped with a DIN concentric cylinder consisting of a rotator spindle with a diameter of 40 mm.

The depletion of NCO groups in pMDI during prepolymerization was determined according to the Test Method B in the ASTM D5155-01. Briefly, 2–4 g of lignin-pMDI prepolymer was added to 75 mL toluene solution containing 50.3 mmol of dibutylamine, followed by adding 10 mL toluene and stirring at 20 °C for 20 min. The solution was then rapidly heated while stirring using a hot plate. After the solution temperature reached 95 °C, the heat was quickly removed and then the solution was allowed to stand for 30 min, followed by adding 225 mL of isopropyl alcohol. Titration was conducted using a 1.0 N HCl to the equivalence point that occurred at the pH level of the solution were between 4.2–4.5. The percent NCO (%NCO) in pMDI after prepolymerization was calculated as follows:

$$\%NCO = 4.202 \times (B–S) / W \quad (3)$$

where B is HCl (mL) required for the titration of a blank sample, S is HCl (mL) for the titration of a prepolymer sample, W is the weight of pMDI in the prepolymer sample. The depletion of NCO (Δ_{NCO}, %) during the prepolymerization was calculated by the following equation:

$$\Delta_{NCO}, \% = (NCO_0 - NCO_1) / NCO_0 \quad (4)$$

where NCO_0 and NCO_1 are the %NCO of pMDI before and after prepolymerization, respectively. With the assumption of all the depleted NCO groups was reacted with lignin OH groups and formed urethane linkages, the percent of reacted OH (Δ_{OH}, %) in lignin during prepolymerization was calculated as follows:

$$\Delta_{OH}, \% = (\Delta_{NCO} \times W_{NCO} \times 7.61) / (W_{lignin} \times 5.33) \quad (5)$$

Table 1
Amounts of components used for the preparation of RPU foams in SIPs.

Lignin amount* (%)	Lignin-pMDI prepolymer			Polyol (g)	NCO index	EffectiveNCO index	ALC* (%)	Cream time (s)	Gel time (s)	Track free time (s)
	pMDI (g)	Silicone oil* (g)	Lignin (g)							
0	120	0	0	120	157	157	0	24	128	186
5	120	0.3	6	120	149	–	2.4	–	–	–
10	120	0.6	12	120	142	152	4.8	27	131	182
15	120	0.9	18	120	135	–	7.0	–	–	–
20	120	1.2	24	120	129	149	9.0	29	130	180
25	120	1.5	30	120	123	–	11.0	–	–	–
30	120	1.8	36	120	118	148	13.0	33	136	180

Notes: *Lignin amount represents to the weight fraction of lignin relative to pMDI in prepolymer. *The amount of silicone oil is 5% respective to the weight of lignin. *ALC is the actual lignin content in RPU foams.

where W_{NCO} and W_{lignin} are the weight (g) of pMDI and lignin in the prepolymer, respectively; 7.61 and 5.33 are the NCO content (mmol/g) in pMDI and OH content (mmol/g) in lignin, respectively.

Since only limited amount of OH groups in lignin could react with isocyanates during prepolymerization, an effective NCO index can be defined as follows, which exclude non-accessible OH groups in lignin:

$$\text{Effective NCO index} = [W_{pMDI} \times NCO_{pMDI} / (W_P \times OH_P + W_{Lig} \times OH_{Lig} \times \Delta_{OH})] \times 100 \quad (6)$$

2.3.2. Physical properties of RPU foams

The apparent density of RPU foams was determined according to ASTM D1622-08. The cell morphology of RPU foams was analyzed by a scanning electron microscopy (SEM, JSM-6110 LV, JOEL). The average cell diameter was estimated from more than 200 measurements by using ImageJ software. The thermal conductivity of RPU foam was measured in z-direction parallel to foam rise direction using a KD2 Pro (Decagon Devices, Inc) thermal conductivity meter. The cross-sectional dimension of RPU foam samples was 50 × 50 mm with a thickness of 100 mm. Ten measurements were conducted for each foam specimen and each measurement was performed over a period of 10 min (Zhang et al., 2018c).

The water absorption of the RPU foams was measured according to ASTM C272 with six replicates. The foam samples had 50 × 50 mm^2 cross-sectional dimension with a thickness of 25 mm. In the water absorption test, the mass and volume of the foam samples were designated as M (g) and V (cm^3), respectively. After immersion into water for 24 h, the weight of samples was designated as N (g). Thus, the water absorption of the samples was calculated as follows: water absorption per unit volume = (N-M) / V.

Thermal stability of RPU foams was evaluated by thermogravimetric analysis (TGA) using a 50H thermo-gravimetric analyzer (TA Instruments). Small pieces of foam (approximately 5 mg) were heated from 50 °C to 750 °C at a ramping rate of 10 °C/min in flowing nitrogen (99.99%, 100 ml/min) atmosphere under ambient pressure.

2.3.3. Mechanical properties of SIPs

The mechanical properties of the as-produced SIPs were measured using the Instron 3382 universal testing machine (Instron Corp.). Depending on the type of testing, the sample size of SIPs under test was varied. The compressive property was measured on eight replicates according to ASTM D1621-10 (crosshead movement rate at 2.5 mm/min). The cross-sectional dimension was 48 × 48 mm^2 with a thickness of 46 mm (Fig. 1a). The stress-strain curves were recorded at a crosshead movement rate of 2.5 mm/min and the compressive strength was determined at the 10% strain point of core foam thickness or at the yield point.

The bonding strength was determined on six replicates through a tension adhesion test according to ASTM D1623-09 (crosshead displacement rate at 0.5 mm/min). The SIP samples for compressive and bonding strength tests had a 50 × 50 mm cross-sectional dimension with a thickness of 46 mm. For bonding strength test, the specimens were adhesively bonded from both sides to a specially prepared steel plate using hot-melt adhesive (Fig. 1b).

The shear strength was measured on six replicates through a tension test according to ASTM C273-16. The specimen had a 100 × 50 mm cross-sectional area with a thickness of 46 mm, which was adhesively bonded from both sides to specially prepared steel plates using hot-melt adhesive (Fig. 1c). The shear test was performed through an extension test at a displacement rate of 0.5 mm/min.

The flexural strength was determined according to the Test Method II of ASTM C203-05a. The specimen was rectangular in cross-section with a width of 38 mm and a length of 355 mm (Fig. 1d). The depth of the specimen was equal to the thickness of the SIP, which was 46 mm. As illustrated in Scheme 1, there are two OSB and core foam interfaces, with one directly formed between the core foam and OSB, and the other one by bonding with an epoxy resin. All SIP samples were tested in the same condition, with the epoxy resin interface being on the bottom when placing a SIP sample on the span. The test was conducted using a midspan loading method and the span was 305 mm. Five replicates were tested at a crosshead displacement rate of 2.5 mm/min.

The foam density, cell size, thermal conductivity, water adsorption, and the mechanical properties of RPU foams and SIPs were analyzed and compared by analysis of variance (ANOVA) using SAS software (SAS Institute, Cary, NC, USA). A one-factor ANOVA with a Fisher's least significant difference (LSD) test was performed to analyze the significance of differences among the sample groups. All statistical analyses were performed at a significance level of 0.05. Standard errors were calculated using the standard deviations of these replicates. Standard error bars were included in all plots.

3. Results and discussion

3.1. Enhancement of lignin interaction with pMDI for RPU foam preparation

Our previous research reported that after prepolymerization treatment at 80 °C for 1 h, some lignin OH groups were reacted with the NCO groups of pMDI through the formation of urethane linkages (Scheme 2) (Zhang et al., 2018c). As shown in Fig. 2, the viscosity (at a shear rate of

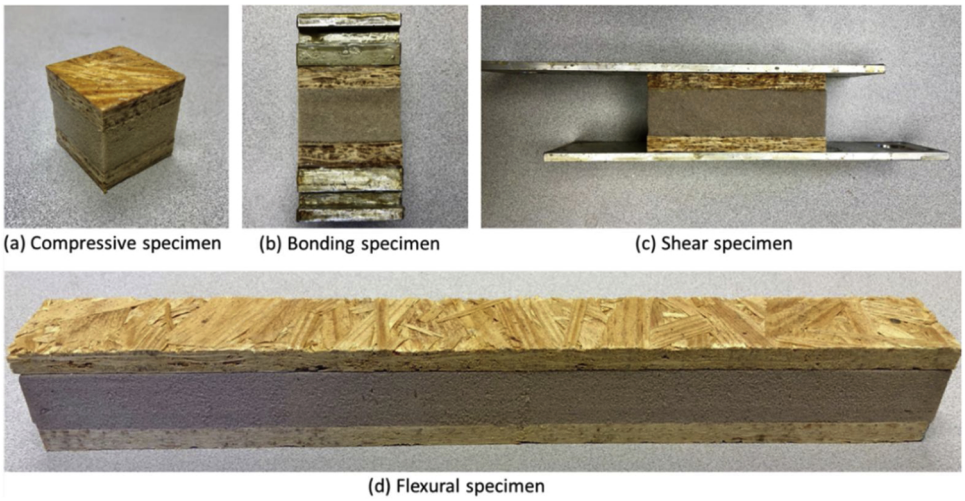

Fig. 1. Configurations of SIP specimens for various mechanical property tests.

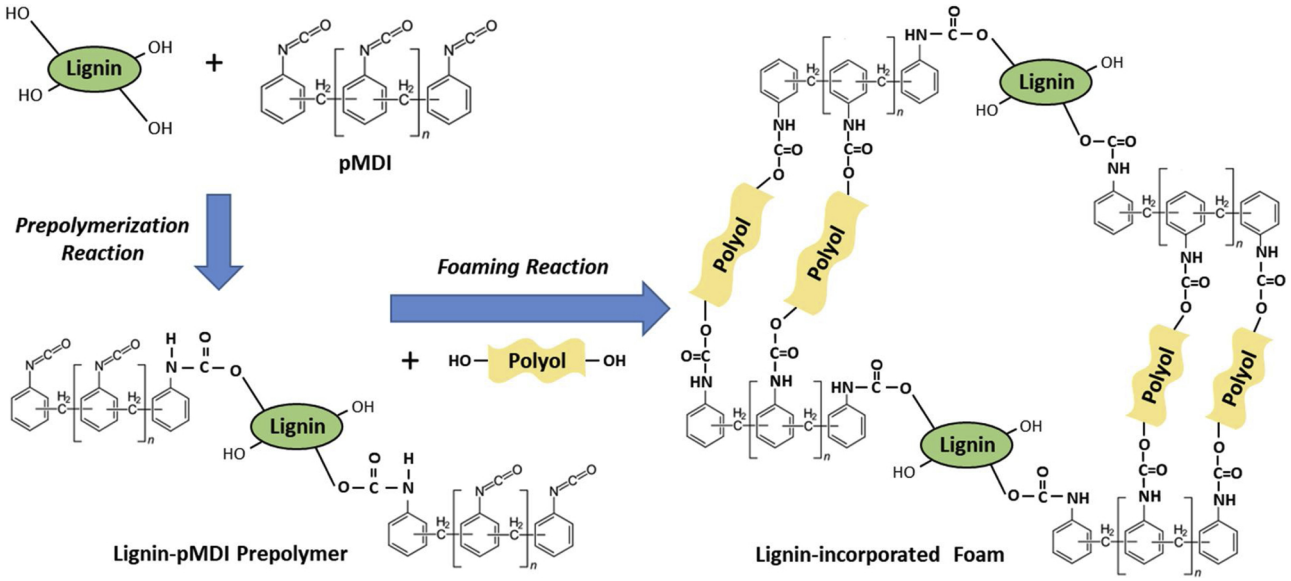

Scheme 2. Reactions during the (a) prepolymerization and (b) foaming processes.

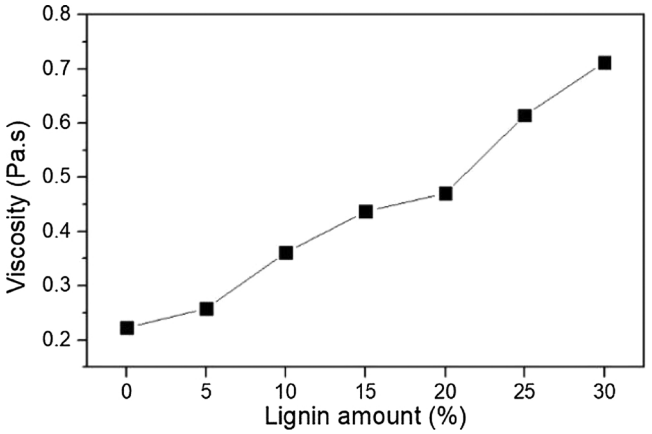

Fig. 2. Viscosity of pMDI alone, and lignin-pMDI prepolymers with up to 30% lignin amount. All data were obtained at a shear rate of 10 s^{-1}.

10 s^{-1}) of the lignin-pMDI prepolymer is strongly dependent on the lignin content in the mixture. The viscosity of the mixture increased from 0.2 to 0.7 Pa·s after adding 30% lignin, which can be attributed to the formation of urethane linkages (pre-crosslinks) between lignin and pMDI and the filler effects of lignin (Chauhan et al., 2014)

In order to determine the amount of modified OH groups in lignin, an amine equivalent wet chemistry experiment was conducted to measure the depletion of NCO groups during the prepolymerization. Our assumption was that, all the NCO groups were consumed through the reaction with lignin OH groups to form urethane linkages. For lignin-pMDI prepolymer containing 10%, 20%, and 30% of lignin, the depletion of NCO groups was found to be 2.1%, 3.5%, and 3.9%, respectively, indicating more urethane linkages (pre-crosslinks) were formed at higher lignin content. On the other hand, for the prepolymer containing 10%, 20%, and 30% of lignin, the amount of modified OH in lignin was found to be 29.7%, 25.3%, and 18.4%, respectively. The decreased in lignin OH modification ratio can be attributed to the agglomeration and aggregation of lignin particles at higher lignin concentration. Limited accessibility of lignin OH groups has been reported previously (Mahmood et al., 2016). Our prepolymerization pretreatment process conducted at 80 °C for 1 h also showed that only 18.4–29.7% of lignin OHs participated in the polyurethane reaction. Given this situation, the unreacted OHs would likely remain inaccessible during the very short time of RPU foam foaming process even with the presence of a catalyst. Therefore, the NCO index from Eq. (1), which considers all OHs in lignin, needs to be modified. When taking into account only the accessible OHs of lignin, the effective NCO index (Eq. (6)) (Table 1) is estimated to be 152, 149, and 148 for the foam with 10%, 20%, and 30% of lignin addition, respectively. Unlike the NCO index, the influence of lignin addition on the effective NCO index in the RPU foams is negligible.

During the foaming process, the reactions among surface modified lignin, pMDI, and polyol occurred simultaneously and produce a foam that crosslinked by these components (Scheme 2). The kinetics of RPU foam formation was investigated by measuring the cream, gel, free rise, and track-free time of RPU foams (Table 1). Cream time shows an increasing trend with the increase of lignin amount (0–30%). This was probably due to the pre-crosslinks between lignin and pMDI, which caused less heat generated at the beginning of foaming reaction and delayed the formation of bubbles. Gel time increased as the amount of lignin increased, which may imply the active interaction of lignin with pMDI (Hayati et al., 2018). Free tracking time decreased with the increase of lignin amount. This can be attributed to the pre-crosslinks between lignin and pMDI, which caused the early termination of the foaming reaction.

3.2. Physical properties of lignin-incorporated RPU foams

The thermal insulation property of a SIP is primarily determined by the physical properties of the core material, *e.g.*, the microstructure and density of the insulating foam. Thus, the cellular structure, apparent density, and thermal conductivity of the RPU foams were first investigated. SEM images of the cross-sections of the RPU foams with different lignin amounts are shown in Fig. 3, displaying the uniformly distributed closed-cell structure of the RPU foams. With the increase in the amount of lignin, cell diameters became progressively smaller. The statistical analysis of the SEM images using ImageJ suggests that the average cell diameter of the RPU foams decreased significantly with increasing amounts of lignin, from 0 to 25% (Table 2). A further increase in the amount of lignin from 25% to 30% did not change the cell diameter. At 25% lignin, the cell diameter had decreased by 63% compared to the reference foam without lignin. The reduced cell diameter is attributed to the facilitation of bubble nucleation by the addition of the lignin during the foaming process (Huang et al., 2018; Luo et al., 2013).

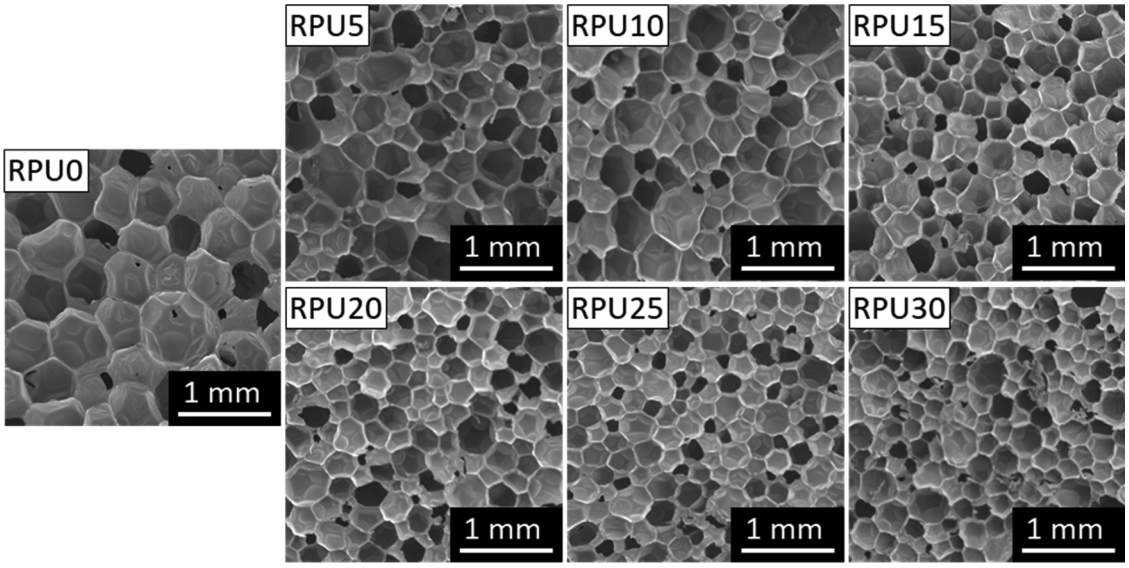

Fig. 3. SEM images of reference and lignin-based (5–30%) RPU foams.

The apparent density and thermal conductivity of the RPU foams are also shown in Table 2. In comparison with the reference foam without lignin, the RPU foams containing 5–10% lignin exhibited markedly lower apparent densities. This result was consistent with the observation of Carriço et al. (2016), which claimed that the addition of lignin improved the nucleation rate of bubbles at an early stage, and thereby, increased the free expansion volume of the foam. There was no significant difference in apparent density between reference foam and RPU foams containing 15% to 25% lignin. However, when the lignin amount increased from 10% to 30%, the apparent densities of the foams progressively increased from 32.3 to 36.5 $kg{\cdot}m^{-3}$, which was even higher than the reference foam. Since the light-weight SIPs are preferred in terms of transportation cost and ease in handling during installation, the low-density RPU foams containing less than 15% of lignin appear to have an advantage for the production of SIPs over the RPU reference foam. Despite the higher apparent densities for the RPU foams containing more than 20% lignin, other advantageous properties may offset the increase in weight, thereby still making them suitable in SIPs.

As mentioned before, the thermal insulation performance of SIPs is dictated by thermal conductivity (κ) of core foams. As shown in Table 2, the κ values of lignin-incorporated RPU foams are in the range of 24.0 to 25.2 $mW{\cdot}m^{-1}K^{-1}$, which meet the thermal conductivity requirements for structural insulation materials specified in ASTM E1730. Compared with the reference foam, the RPU foams containing up to 25% lignin showed no significant difference in thermal conductivity except that containing 30% lignin with its higher κ value.

SIPs are mainly used as structural and functional components in walls, roofs, and floors for residential and commercial buildings. When exposed to high humidity conditions during use, the structural durability and thermal insulation property of SIPs will be a critical concern. Water resistance of RPU foams is an important property because the absorbed water and moisture not only deteriorate overall structural durability but also decrease the thermal insulation property of RPU foams (Avilés and Aguilar-Montero, 2010; Huo et al., 2016), which will eventually affect the mechanical and thermal performance of SIPs. As shown in Table 2, the water absorption of all RPU foams was below 2.0×10^{-2} g/cm^3, which is indeed much lower than the maximum water adsorption limit of 4.3×10^{-2} g/cm^3 specified in ANSI/APA PRS 610.1–2013 for polyurethane insulation materials. The statistical analysis also confirmed that the addition of lignin does not affect the water adsorption of the resultant foams. Since lignin is a hydrophobic polymer, is was anticipated that its addition would not change the water absorption capability of the RPU foams. It was reported that the water absorption of RPU foams can be affected by their cell structure. Generally, the larger the cell diameter, the more water absorption of RPU foams because larger cells will be able to accommodate more water (Thirumal et al., 2008). However, as shown in SEM images in Fig. 3, the cell diameter of the RPU foams decreased with increasing lignin amounts, while the water absorption of all the RPU foams remains the same. It is believed that the foams with higher lignin amounts may contain more broken cells, and thereby, contribute to greater water absorption through cell interconnections.

Fig. 4 shows thermogravimetric (TG) and derivative thermogravimetric (dTG) curves of the RPU foams. All of the foam samples were degraded in a broad temperature range of 150–650 °C (with the

Table 2
The cell diameter, apparent density, and thermal conductivity and water adsorption of reference and lignin-based RPU foams.

Lignin amount (%)*	Cell diameter (μm)	Apparent density ($kg{\cdot}m^{-3}$)	Thermal conductivity ($mW{\cdot}m^{-1}{\cdot}K^{-1}$)	Water absorption ($g/cm^3 \times 10^{-2}$)	Char yield at 700 °C (%)
0	588 ± 85* A*	34.6 ± 1.8 A,D	24.2 ± 0.7 A	1.82 ± 0.27 A	20.7
5	366 ± 112 B	31.4 ± 0.6 B	24.7 ± 0.2 A,B	1.91 ± 0.28 A	21.3 (21.3*)
10	355 ± 129 C	32.3 ± 1.1 B,C	24.5 ± 0.5 A,B	1.81 ± 0.25 A	22.5 (21.8)
15	284 ± 75 D	33.4 ± 0.8 C,D	24.5 ± 0.8 A,B	1.77 ± 0.18 A	23.0 (22.3)
20	246 ± 57 E	34.5 ± 1.3 A,D	24.0 ± 0.1 A	1.83 ± 0.15 A	25.9 (22.8)
25	220 ± 43 F	35.1 ± 1.4 A	24.0 ± 0.1 A	1.86 ± 0.15 A	27.8 (23.3)
30	216 ± 55 F	36.5 ± 1.0 E	25.2 ± 1.0 B	1.97 ± 0.39 A	28.0 (23.7)

Notes: *Lignin amount represents to the weight fraction of lignin relative to pMDI in prepolymer. *Values are averages with standard deviations. *Different letters in each column indicate statistically significant differences between groups ($p < 0.05$, LSD test). *Numbers in parentheses are calculated values of char yields based on the principle of additivity.

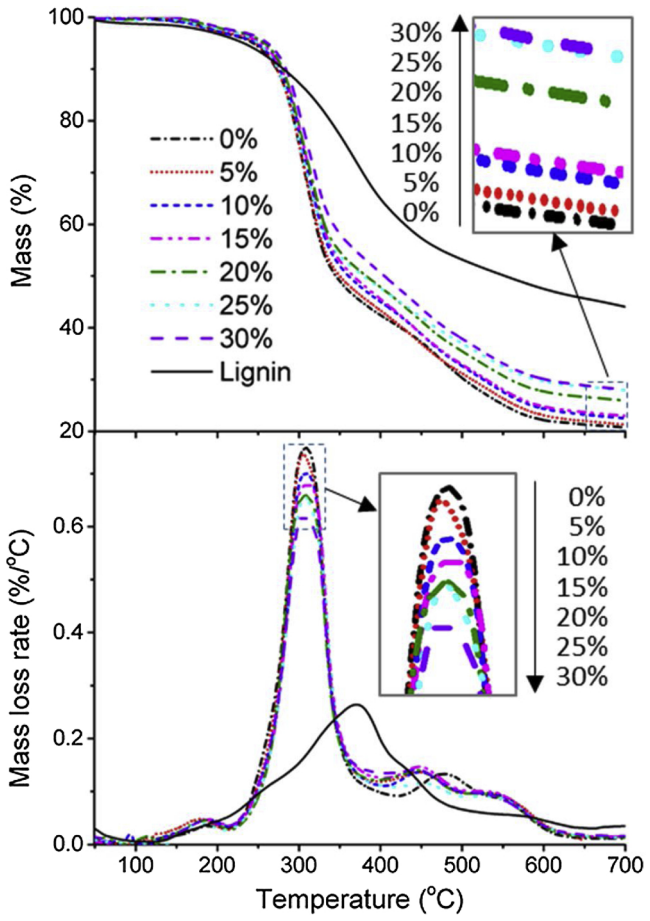

Fig. 4. TG and dTG curves of lignin and the RPU foams with different amount (0%–30%) of lignin.

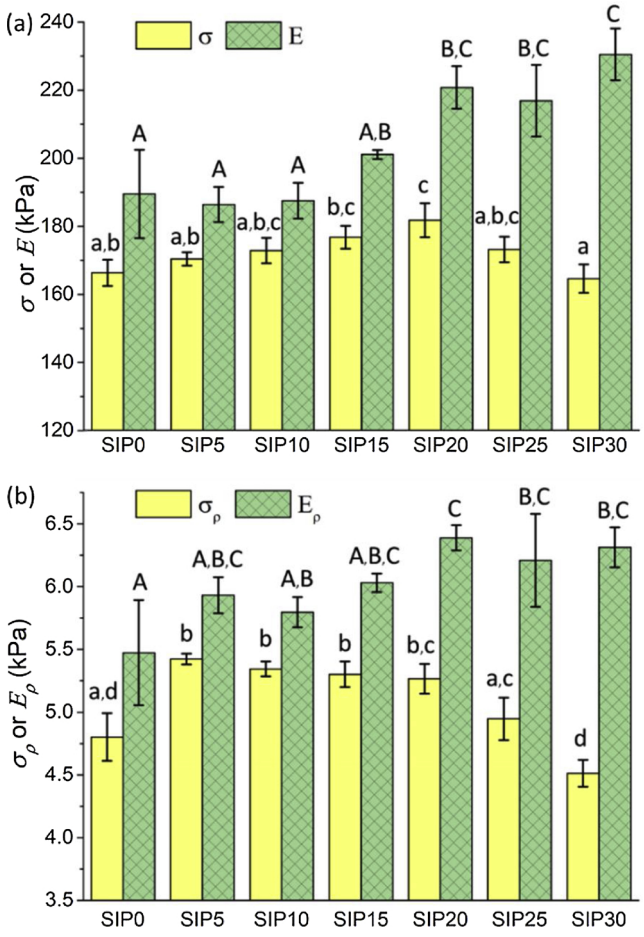

Fig. 5. Compressive properties of the SIPs containing reference and lignin-based RPU foams as a core: (a) compressive strength (σ) and compressive modulus (E); (b) specific compressive strength (σ_ρ) and specific compressive modulus (E_ρ). Different letters indicate statistically significant differences between groups ($p < 0.05$, LSD test).

maximum dTG peak at ˜308 °C). As the amount of lignin increased from 0 to 30%, the char yield of RPU foams at 700 °C increased from 20.7% to 28.0%, while the maximum mass loss rate (dTG_{max}) showed a decreasing trend. These phenomena indicated thermal stability of RPU foams was enhanced by the addition of lignin. This was because lignin is a thermostable polymer (Gómez-Fernández et al., 2018), which has much higher char yield (44%) and dTG_{max} temperature (371 °C) than that of reference foam, as shown in Fig.4. In the case of all lignin-incorporated RPU foams, the char yield is higher than that predicted by the principle of additivity (Table 2), indicating that the improved thermal stability can be also attributed the formation of the highly cross-linked thermostable segments arising from the interactions between lignin and the RPU foam matrix. The increased crosslink density of RPU foams was also confirmed by the FTIR spectra (Figs S3 and S4 in SI).

3.3. Mechanical properties of SIPs

3.3.1. Compressive properties

SIPs show similar structural characteristics with a steel I-beam, in which the OSB faces serve as a flange and the RPU foam core functions as a web that is designed to withstand in-plane compressive loads (Jing and Raongjant, 2013). Thus, the compressive strength of SIPs is determined by that of the RPU foam core. As shown in Fig. 5a, all the SIPs with a lignin-incorporated RPU foam core in this study exhibited compressive strength (σ) of 165 to 182 kPa and compressive modulus (E) of 185 to 235 kPa, which meet the compressive strength requirements specified in ANSI/APA PRS 610.1–2013 for wood construction applications. Note that letters above columns in Fig. 5a indicate statistical grouping from ANOVA with an LSD test. This shows that the addition of lignin can have a significant effect on the σ and E of SIPs. As the addition of lignin increased to 20%, both σ and E increased. This enhancement can be attributed to the greater crosslinking density of RPU foams due to the addition of lignin (Luo et al., 2013). Further increase in lignin amount (20% to 30%) resulted in a significant decrease in σ but an increase in E. The lowest σ at 30% lignin content can be attributed to the agglomeration and aggregation of lignin particles in cell walls of the foam, which is likely to occur at a higher lignin concentration. The decline in compressive strength of RPU foams with the reduced lignin dispersion in the foam was also reported previously (Pan and Saddler, 2013). The increase in E over a wide range of lignin content (0–30%) indicates the addition of lignin increased the rigidity of RPU foams. It is worthwhile to note that the apparent density of the RPU foams increased when lignin content was greater than 20% (Table 2). It is well known that the compressive strength and modulus of SIP's core foam are closely related to the apparent density of the foam (Carriço et al., 2016; Paruzel et al., 2017).

As described before, the apparent density of core RPU foam varies with lignin amount. Thus, normalized compressive strength (σ_ρ, compressive strength per unit density) and modulus (E_ρ, compressive modulus per unit density) were used to compare the effect of lignin on the compressive properties (Fig. 5b) of lignin-incorporated SIPs. The SIPs with lignin amount up to 20% showed significantly higher σ_ρ by 13% at maximum in comparison with the reference SIP (SIP0). This improvement in normalized compressive strength would be combined

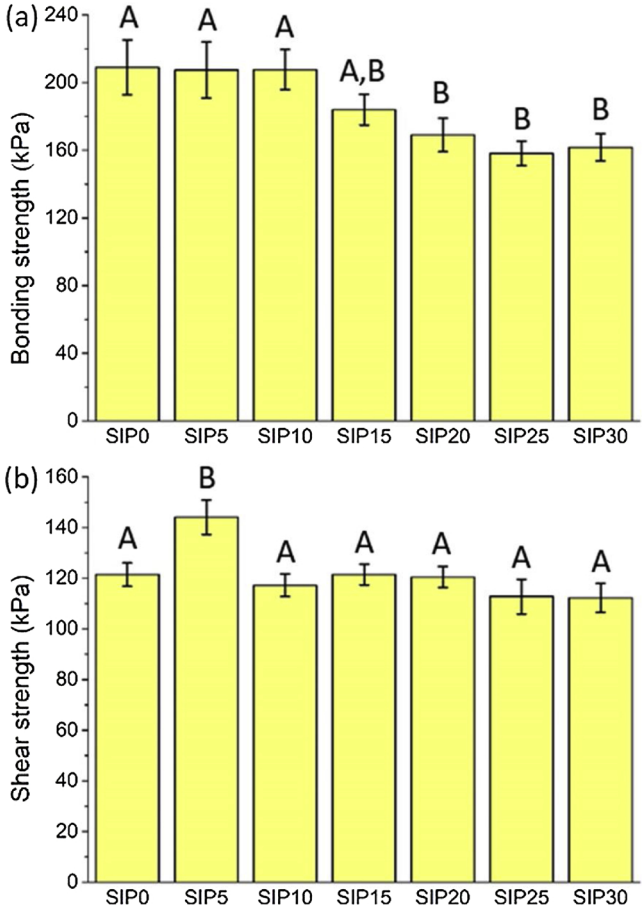

Fig. 6. (a) Bonding and (b) shear strength of reference and lignin-based SIPs. Different letters indicate statistically significant differences between groups ($p < 0.05$, LSD test).

effects of reduced apparent density, and the increased crosslinking density of the foams. As same as σ in Fig. 5a, further increase in lignin content from 20% to 30% resulted in a significant reduction in σ_ρ. Since E_ρ exhibited the same trend to E, this further suggested an enhancement effect of the lignin in the RPU foams.

3.3.2. Bonding and shear strength of SIPs

Fig. 6a shows that bonding strength of SIPs with different lignin amount is between 158 and 209 kPa. The reader should recall that one interface is that where the foam is directly bonded to the OSB, while the other involves bonding of the OSB to the formed rigid foam with an epoxy resin. In all cases, the failure occurred at the interface having the foam directly bonded to the OSB during foam curing. This indicates that the self-adhesion of the foam to the OSB was not as strong as the bond with the epoxy resin. The RPU foams containing more than 15% lignin content show lower bonding strength than the reference, which is also supported by ANOVA results. Compared to the reference, reduction in bonding strength of RPU foam was 19.1% and 22.3%, at 20% and 30% lignin amounts, respectively. Reduced bonding strength can be attributed to the increased viscosity of PU precursors when lignin was added, which resulted in the limited penetration of the precursors into OSB (Cheng and Sun, 2006). It should be noted that despite some degree of reduction in bonding strength, all lignin-incorporated SIPs meet the bonding strength requirements specified in ANSI/APA PRS 610.1–2013 for construction wall applications.

Fig. 6b shows shear strength of the SIPs to vary lignin amount. Note that the shear strength of a SIP is affected by the adhesion between the OSB layers and core foams, as well as shear resistance of core foams. For the SIP with the reference foam (SIP0) and the 5% lignin RPU foam (SIP5), failure resulted from shear within the core foams. When lignin amount in the RPU foam was higher than 5%, the failure mainly occurred near the interface between OSB and core foam. Again, there are two OSB and core foam interfaces, with one where the foam is directly bonded to the OSB and the other where the OSB is bonded to the formed rigid foam with an epoxy resin. In all cases where failures occurred at an interface, it was that interface having the foam directly bonded to the OSB during foam curing. It is interesting to note that the SIP with 5% lignin exhibited significantly higher shear strength than the reference SIP and the other lignin-incorporated SIPs (see Fig. 6b). The increased shear strength of SIP5 can be attributed to the improvement effect of lignin on shear resistance of the core foams. However, despite the strengthening effect of lignin, the SIPs with the highest amounts of lignin may suffer reduced bonding strength, which, we believe is reflected in overall similar shear strengths of all the SIPs except SIP5.

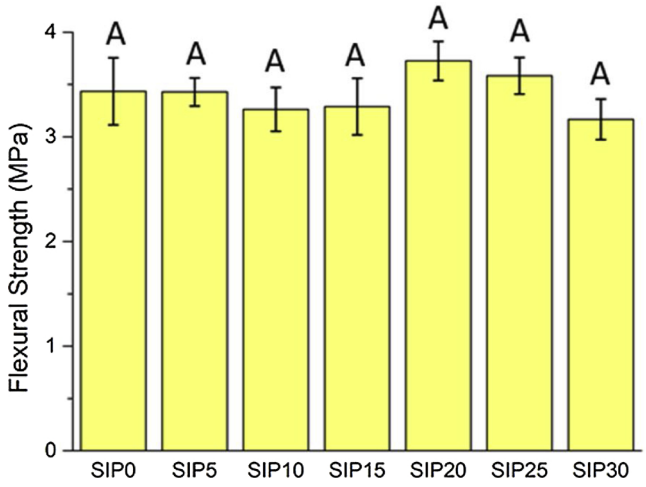

Fig. 7. Flexural strength of reference and lignin-based SIPs. Different letters indicate statistically significant differences between groups ($p < 0.05$, LSD test).

3.3.3. Flexural strength of SIPs

The effect of lignin amount on the flexural strength of SIPs is presented in Fig. 7. Several factors have been thought to affect the flexural strength of SIPs, which include the density and mechanical strength of OSB layers, adhesion between OSB layers and core foams, and density and strength of core foams (Shalbafan et al., 2012). In this study, all rupture failure was found to occur within the OSB faces, except for several samples from SIP30, in which the fracture occurred simultaneously in OSB faces and core foams. As shown in Fig. 7, the flexural strength of all SIPs with up to 30% lignin were essentially the same with no significant difference being observed by ANOVA. The many factors that contributed to the flexural strength of SIPs involve interplay between the foam-to-OSB interfaces and the compressive/tensile properties of individual components. Although the ANOVA results suggested the addition of lignin to the RPU foam up to the 30% amount did not negatively impact the flexural strengths of the SIPs, additions of lignin above 25% are not recommended on the basis of the foam failures that accompanied the OSB failures at the 30% lignin amount.

4. Conclusions

Lab-scale SIPs were constructed using lignin-incorporated RPU foams as a thermal insulation core. Surface-functionalization of the lignin improved its function as a reactive crosslinker filler through enhancing the interaction between lignin and pMDI and minimizing inhomogeneous dispersion of the lignin in the mixture of RPU components. The addition of lignin in the RPU foams led to increasing levels of

thermal stability and similar thermal insulation and water absorption performance. The SIPs prepared with lignin-incorporated RPU foams as a core showed increased compressive strength and modulus by 9% and 17%, as compared to the reference SIPs. Other mechanical properties of the SIPs containing lignin-incorporated RPU foams, such as bonding, shear, and flexural strength, were comparable or marginally decreased, but still met requirements in industrial specifications for building and construction. Overall, the amount of lignin addition between 5%–15% is recommended. This study represents a facile approach to utilize lignin as a component in a sandwich structure composite that has broad implications as a building material. Future work is planned to construct the industrial-scale SIPs with the lignin-incorporated RPU foams as a thermal insulation core, with the aim of making an immediate impact on the building industry.

Acknowledgments

This work was supported by the U.S. Forest Service, Wood Education and Resource Center (WERC), Wood Innovations Grant, No. 16-DG-11083150-052. The authors would like to acknowledge Ingevity Corp., South Carolina for providing kraft lignin for this study and Dr. Xingyan Huang at Louisiana State University for his assistance in the experiments. This manuscript is publication #SB938 of the Department of Sustainable Bioproducts, Mississippi State University.

Appendix A. Supplementary data

Supplementary data associated with this article can be found, in the online version, at https://doi.org/10.1016/j.indcrop.2019.02.035.

References

Amaral, J.S., Sepúlveda, M., Cateto, C.A., Fernandes, I.P., Rodrigues, A.E., Belgacem, M.N., Barreiro, M.F., 2012. Fungal degradation of lignin-based rigid polyurethane foams. Polym. Degrad. Stab., 3rd International Conference on Biodegradable and Biobased Polymers (BIOPOL-2011) - Strasbourg 2011 97, 2069–2076. https://doi.org/10.1016/j.polymdegradstab.2012.03.037.

Avilés, F., Aguilar-Montero, M., 2010. Moisture absorption in foam-cored composite sandwich structures. Polym. Compos. 31, 714–722. https://doi.org/10.1002/pc.20872.

Bartel, R., 2018. SIPs vs. Sticks; Contractors' Guide to Using SIPs [WWW Document]. URL (Accessed 10.1.18). https://www.enercept.com/blog/sips-vs-sticks-contractors-guide-to-using-sips.

Bernardini, J., Cinelli, P., Anguillesi, I., Coltelli, M.-B., Lazzeri, A., 2015. Flexible polyurethane foams green production employing lignin or oxypropylated lignin. Eur. Polym. J. 64, 147–156. https://doi.org/10.1016/j.eurpolymj.2014.11.039.

Carriço, C.S., Fraga, T., Pasa, V.M.D., 2016. Production and characterization of polyurethane foams from a simple mixture of castor oil, crude glycerol and untreated lignin as bio-based polyols. Eur. Polym. J. 85, 53–61. https://doi.org/10.1016/j.eurpolymj.2016.10.012.

Cateto, C., Barreiro, F., Rodrigues, A., Belgacem, N., 2008. Rigid polyurethane foams from lignin based-polyols. AIP Conf. Proc. 1042, 243–245. https://doi.org/10.1063/1.2989020.

Cateto, C.A., Barreiro, M.F., Ottati, C., Lopretti, M., Rodrigues, A.E., Belgacem, M.N., 2014. Lignin-based rigid polyurethane foams with improved biodegradation. J. Cell. Plast. 50, 81–95. https://doi.org/10.1177/0021955X13504774.

Chauhan, M., Gupta, M., Singh, B., Singh, A.K., Gupta, V.K., 2014. Effect of functionalized lignin on the properties of lignin–isocyanate prepolymer blends and composites. Eur. Polym. J. 52, 32–43. https://doi.org/10.1016/j.eurpolymj.2013.12.016.

Cheng, E., Sun, X., 2006. Effects of wood-surface roughness, adhesive viscosity and processing pressure on adhesion strength of protein adhesive. J. Adhes. Sci. Technol. 20, 997–1017. https://doi.org/10.1163/156856106777657779.

Choi, H.-J., Kang, J.-S., Huh, J.-H., 2018. A study on variation of thermal characteristics of insulation materials for buildings according to actual long-term annual aging variation. Int. J. Thermophys. 39 (2). https://doi.org/10.1007/s10765-017-2318-3.

FAS, 2010. Expanding the Scope and Market of SIP Technologies: A history of SIPs and CSIP Manufacturing (Construction and Market Issues). Federation of American Scientists.

Gómez-Fernández, S., Ugarte, L., Calvo-Correas, T., Peña-Rodríguez, C., Corcuera, M.A., Eceiza, A., 2017. Properties of flexible polyurethane foams containing isocyanate functionalized kraft lignin. Ind. Crops Prod. 100, 51–64. https://doi.org/10.1016/j.indcrop.2017.02.005.

Gómez-Fernández, S., Günther, M., Schartel, B., Corcuera, M.A., Eceiza, A., 2018. Impact of the combined use of layered double hydroxides, lignin and phosphorous polyol on the fire behavior of flexible polyurethane foams. Ind. Crops Prod. 125, 346–359. https://doi.org/10.1016/j.indcrop.2018.09.018.

Hayati, A.N., Evans, D.A.C., Laycock, B., Martin, D.J., Annamalai, P.K., 2018. A simple methodology for improving the performance and sustainability of rigid polyurethane foam by incorporating industrial lignin. Ind. Crops Prod. 117, 149–158. https://doi.org/10.1016/j.indcrop.2018.03.006.

Huang, X., De Hoop, C.F., Xie, J., Wu, Q., Boldor, D., Qi, J., 2018. High bio-content polyurethane (PU) foam made from bio-polyol and cellulose nanocrystals (CNCs) via microwave liquefaction. Mater. Des. 138, 11–20. https://doi.org/10.1016/j.matdes.2017.10.058.

Huo, Z., Mohamed, M., Nicholas, J.R., Wang, X., Chandrashekhara, K., 2016. Experimentation and simulation of moisture diffusion in foam-cored polyurethane sandwich structure. J. Sandw. Struct. Mater. 18, 30–49. https://doi.org/10.1177/1099636215582218.

Jing, M., Raongjant, W., 2013. Using GFRP to develop the mechanical performance of structural insulated panels. Adv. Mater. Res. 1941–1944. https://doi.org/10.4028/www.scientific.net/AMR.671-674.1941. 671–674.

Kirpluks, M., Kalnbunde, D., Benes, H., Cabulis, U., 2018. Natural oil based highly functional polyols as feedstock for rigid polyurethane foam thermal insulation. Ind. Crops Prod. 122, 627–636. https://doi.org/10.1016/j.indcrop.2018.06.040.

Li, Y., Ragauskas, A.J., 2012. Kraft lignin-based rigid polyurethane foam. J. Wood Chem. Technol. 32, 210–224. https://doi.org/10.1080/02773813.2011.652795.

Li, H., Feng, S., Yuan, Z., Wei, Q., Xu, C.C., 2017. Highly efficient liquefaction of wheat straw for the production of bio-polyols and bio-based polyurethane foams. Ind. Crops Prod. 109, 426–433. https://doi.org/10.1016/j.indcrop.2017.08.060.

Luo, X., Mohanty, A., Misra, M., 2013. Lignin as a reactive reinforcing filler for water-blown rigid biofoam composites from soy oil-based polyurethane. Ind. Crops Prod. 47, 13–19. https://doi.org/10.1016/j.indcrop.2013.01.040.

Mahmood, N., Yuan, Z., Schmidt, J., Xu, C., 2016. Depolymerization of lignins and their applications for the preparation of polyols and rigid polyurethane foams: a review (Charles). Renewable Sustainable Energy Rev. 60, 317–329. https://doi.org/10.1016/j.rser.2016.01.037.

Nadji, H., Bruzzèse, C., Belgacem, M.N., Benaboura, A., Gandini, A., 2005. Oxypropylation of lignins and preparation of rigid polyurethane foams from the ensuing polyols. Macromol. Mater. Eng. 290, 1009–1016. https://doi.org/10.1002/mame.200500200.

Pan, X., Saddler, J.N., 2013. Effect of replacing polyol by organosolv and kraft lignin on the property and structure of rigid polyurethane foam. Biotechnol. Biofuels 6 (12). https://doi.org/10.1186/1754-6834-6-12.

Paruzel, A., Michałowski, S., Hodan, J., Horák, P., Prociak, A., Beneš, H., 2017. Rigid polyurethane foam fabrication using medium chain glycerides of coconut oil and plastics from end-of-life vehicles. ACS Sustain. Chem. Eng. 5, 6237–6246. https://doi.org/10.1021/acssuschemeng.7b01197.

Septevani, A.A., Evans, D.A.C., Annamalai, P.K., Martin, D.J., 2017. The use of cellulose nanocrystals to enhance the thermal insulation properties and sustainability of rigid polyurethane foam. Ind. Crops Prod. 107, 114–121. https://doi.org/10.1016/j.indcrop.2017.05.039.

Shalbafan, A., Luedtke, J., Welling, J., Fruehwald, A., 2012. Physiomechanical properties of ultra-lightweight foam core particleboard: different core densities. Holzforschung 67, 169–175. https://doi.org/10.1515/hf-2012-0058.

Thirumal, M., Khastgir, D., Singha, N.K., Manjunath, B.S., Naik, Y.P., 2008. Effect of foam density on the properties of water blown rigid polyurethane foam. J. Appl. Polym. Sci. 108, 1810–1817. https://doi.org/10.1002/app.27712.

Xue, B.-L., Wen, J.-L., Sun, R.-C., 2014. Lignin-based rigid polyurethane foam reinforced with pulp fiber: synthesis and characterization. ACS Sustain. Chem. Eng. 2, 1474–1480. https://doi.org/10.1021/sc5001226.

Zhang, X., Yan, Q., Leng, W., Li, J., Zhang, J., Cai, Z., Hassan, E.B., 2017. Carbon nanostructure of kraft lignin thermally treated at 500 to 1000 °C. Materials 10, 975. https://doi.org/10.3390/ma10080975.

Zhang, X., Jeremic, D., Kim, Y., Street, J., Shmulsky, R., 2018a. Effects of surface functionalization of lignin on synthesis and properties of rigid bio-based polyurethanes foams. Polymers 10, 706. https://doi.org/10.3390/polym10070706.

Zhang, X., Yan, Q., Li, J., Chu, I.-W., Toghiani, H., Cai, Z., Zhang, J., 2018b. Carbon-based nanomaterials from biopolymer lignin via catalytic thermal treatment at 700 to 1000 °C. Polymers 10, 183. https://doi.org/10.3390/polym10020183.

Zhang, X., Yan, Q., Li, J., Zhang, J., Cai, Z., 2018c. Effects of physical and chemical states of iron-based catalysts on formation of carbon-encapsulated iron nanoparticles from kraft lignin. Materials 11, 139. https://doi.org/10.3390/ma11010139.